

Adaptive Depth Networks with Skippable Sub-Paths

Woochul Kang

Department of Embedded Systems

Incheon National University

119 Academy-Ro, Yeonsu-Gu, Incheon, South Korea

wchkang@inu.ac.kr

Abstract

Systematic adaptation of network depths at runtime can be an effective way to control inference latency and meet the resource condition of various devices. However, previous depth adaptive networks do not provide general principles and a formal explanation on why and which layers can be skipped, and, hence, their approaches are hard to be generalized and require long and complex training steps. In this paper, we present an architectural pattern and training method for adaptive depth networks that can provide flexible accuracy-efficiency trade-offs in a single network. In our approach, every residual stage is divided into 2 consecutive sub-paths with different properties. While the first sub-path is mandatory for hierarchical feature learning, the other is optimized to incur minimal performance degradation even if it is skipped. Unlike previous adaptive networks, our approach does not iteratively self-distill a fixed set of sub-networks, resulting in significantly shorter training time. However, once deployed on devices, it can instantly construct sub-networks of varying depths to provide various accuracy-efficiency trade-offs in a single model. We provide a formal rationale for why the proposed architectural pattern and training method can reduce overall prediction errors while minimizing the impact of skipping selected sub-paths. We also demonstrate the generality and effectiveness of our approach with various residual networks, both from convolutional neural networks and vision transformers.

1. Introduction

Modern deep neural networks such as convolutional neural networks (CNNs) and transformers [44] provide state-of-the-art performance at high computational costs, and, hence, lots of efforts have been made to leverage those inference capabilities in various resource-constrained devices. Those efforts include compact architectures [13, 21], network pruning [14, 33], weight/activation quantization [26], knowledge distillation [19], to name a few. However,

those approaches provide static accuracy-efficiency trade-offs, and, hence, it is infeasible to deploy one single model to meet devices with all kinds of resource-constraints.

There have been some attempts to provide predictable adaptability to neural networks by exploiting the redundancy in either network depths [6, 24], widths [48, 59], or both [20, 47]. However, one major difficulty with prior adaptive networks is that they are hard to train and require significantly longer training time than non-adaptive networks. For example, most adaptive networks select a fixed number of sub-networks of varying depths or width, and train them iteratively, mostly through self-distilling knowledge from the largest sub-network (also referred to as the *super-net*) [20, 43, 48, 59]. However, this iterative self-distillation takes long time and can generate conflicting training objectives for different parameter-sharing sub-networks, potentially resulting in worse performance [10, 30]. Further, unlike width-adaptation networks, no general principle has been proposed for how to select sub-networks for depth adaptation, since the effect of skipping individual layers has not been formally specified.

In this work, we introduce an architectural pattern and training method for adaptive depth networks that is generally applicable to residual networks, e.g., CNNs and transformers. In the proposed adaptive depth networks, every residual stage is divided into 2 consecutive sub-paths and they are trained to have different properties. While the first sub-paths are mandatory for hierarchical feature learning, the second sub-paths are optimized to incur minimal performance degradation even if they are skipped. More specifically, the second sub-path of every residual stage is optimized to preserve the feature distribution from its previous mandatory sub-path in order to minimize the performance degradation when it is skipped. During training, this property of the second sub-paths is enforced through *skip-aware self-distillation*, in which only one smallest sub-network, also referred as the *base-net*, is jointly trained in order to self-distill intermediate feature distributions at every residual stage, as shown in Figure-1-(a). This skip-aware self-

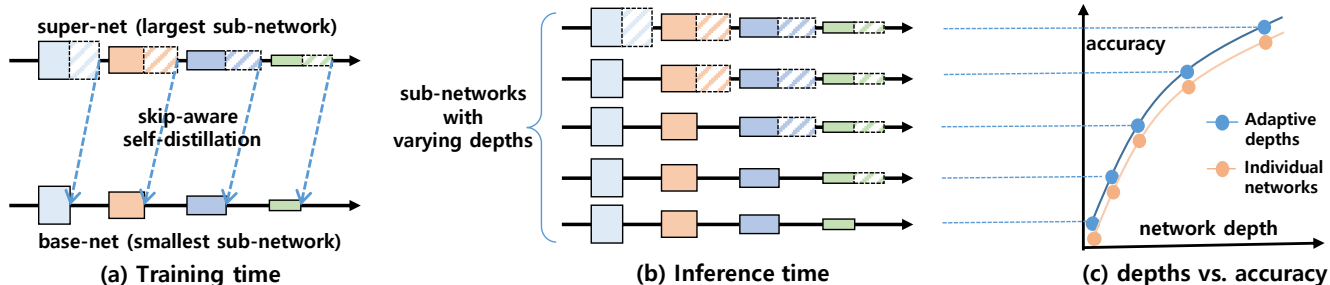


Figure 1. (a) At training time, the last half layers of every residual stage is optimized to have minimal performance degradation even if they are skipped. No explicit self-distillation is required for sub-networks, except the smallest base-net. (b) At test time, 2^{N_r} sub-networks become available in a single network by systematically skipping last half layers of N_r residual stages. (c) Sub-networks instantly selected from a single network outperform counterpart individually trained networks due to regularization effect.

distillation requires no explicit self-distillation or additional fine-tuning of individual sub-networks except the base-net, resulting in significantly shorter training time than previous adaptive networks. However, once trained, sub-networks with various depths can be selected instantly from a single network to meet the resource condition of devices, as shown in Figure 1-(b). Further, these sub-networks with various depths outperform individually trained non-adaptive networks due to the regularization effect, as shown in Figure 1-(c).

In Section 3, we discuss the details of our architectural pattern and training algorithm, and show formally that the chosen sub-paths trained with our skip-aware self-distillation are optimized to reduce prediction errors while minimally changing the level of input features. In Section 4, we empirically demonstrate that our adaptive depth networks with skippable sub-paths outperform counterpart individual networks, both in CNNs and vision transformers, and achieve actual inference acceleration and energy-saving.

To authors’ best knowledge, this work is the first general approach to adaptive depth networks, providing a general principle for depth adaptation and a formal explanation on why layers can be skipped with minimal performance degradation.

2. Related Work

Adaptive Networks: In most adaptive networks, parameter-sharing sub-networks are selected by adjusting either widths, depths, or resolutions [3, 20, 22, 24, 30, 47, 48, 59, 61]. For example, slimmable neural networks adjust channel widths of CNN models on the fly for accuracy-efficiency trade-offs and they exploit switchable batch normalization to handle multiple sub-networks [48, 58, 59]. Transformer-based adaptive depth networks have been proposed for language models to dynamically skip some of the layers during inference [6, 20]. However, in these adaptive networks, every target

sub-network with varying widths or depths need to be trained explicitly, incurring significant training overheads and potential conflicts between sub-networks.

Dynamic networks [15] are another class of adaptive networks that exploit additional control networks or decision gates for input-dependent adaption of CNN models [12, 29, 31, 51, 53] and transformers [8, 18, 35, 55]. In particular, most dynamic networks for depth-adaptation have some kinds of decision gates at every layers (or blocks) that determine if the layers can be skipped [9, 45, 50, 51]. These approaches are based on the thought that some layers can be skipped on ‘easy’ inputs. However, the learned policy for skipping layers is opaque to users and does not provide a formal description of when and which layers can be skipped for a given input. Therefore, the network depths cannot be adapted in a predictable manner to meet the resource condition of target devices.

Residual Blocks with Shortcuts: Since the introduction of ResNets [16], residual blocks with shortcuts have received extensive attention because of their ability to train very deep networks, and have been chosen by many CNNs [38, 41] and transformers [5, 34, 44]. In [46], Veit et al. argue that identity shortcuts make exponential paths and results in an ensemble of shallower sub-networks. This thought is supported by the fact that removing individual residual blocks at test time does not significantly affect performance, and it has been further exploited to train deep networks [23, 52]. Other works argue that identity shortcuts enable residual blocks to perform iterative feature refinement, where each block improves slightly but keeps the semantic of the representation of the previous layer [11, 27]. Our work build upon those views on residual blocks with shortcuts and further extend them for adaptive depth networks by introducing an architectural pattern and training method that exploits the properties of residual blocks more explicitly for selected sub-paths.

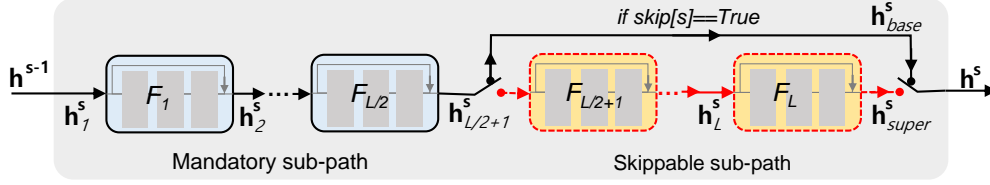


Figure 2. Illustration of a residual stage with 2 sub-paths. While the first sub-path is mandatory for hierarchical feature learning, the second (yellow) sub-path can be skipped for efficiency. The layers in the skippable sub-path are trained to preserve the feature distribution from \mathbf{h}_{base}^s to \mathbf{h}_{super}^s using *skip-aware self-distillation*. Having similar feature distributions, either \mathbf{h}_{base}^s or \mathbf{h}_{super}^s can be provided as an input to the next residual stage. In the mandatory sub-path, another set of batch normalization operators, called *skip-aware BNs*, is exploited when the second sub-path is skipped. This architectural pattern repeats in every residual stage throughout the network.

3. Adaptive Depth Networks

We first present an architectural pattern and training details to build adaptive depth networks. And, then, we discuss the theoretic rationale for how depth adaption can be achieved with minimal performance degradation.

3.1. Architectural Pattern for Depth Adaptation

In typical hierarchical residual networks such as ResNets [16] and Swin transformers [34], the s -th residual stage is consisted of L identical residual blocks, which transform input features \mathbf{h}_1^s additively to produce the output features \mathbf{h}^s , as follows:

$$\mathbf{h}_1^s + \underbrace{F_1(\mathbf{h}_1^s) + \dots + F_{L/2}^s(\mathbf{h}_{L/2}^s)}_{\mathbf{F}_{base}^s} + \underbrace{\dots + F_L(\mathbf{h}_L^s)}_{\mathbf{F}_{skippable}^s} = \mathbf{h}^s$$

$$\underbrace{\hspace{10em}}_{=\mathbf{h}_{base}^s}$$

$$\underbrace{\hspace{15em}}_{=\mathbf{h}_{super}^s} \quad (1)$$

While a block with a residual function F_ℓ ($\ell = 1, \dots, L$) learns hierarchical features as traditional compositional networks [40], previous literature [11, 27] demonstrates that a residual function also tend to learn a function that refines already learned features at the same feature level. If a residual block mostly performs feature refinement while not changing the level of input features, the performance of the residual network is not significantly affected by dropping the block at test time [23, 52]. However, in typical residual networks, most residual blocks tend to refine features while learning new level features as well, and, hence, random dropping of residual blocks at test time degrades the performance significantly. Therefore, we hypothesize that if some designated residual blocks can be encouraged during training to focus more on feature refinement, then these blocks can be skipped to save computation at marginal loss of prediction accuracy at test time.

To this end, we propose an architectural pattern for adaptive depth networks, in which every residual stage is divided into two consecutive sub-paths, or \mathbf{F}_{base}^s and $\mathbf{F}_{skippable}^s$ as

in Equation 1 and Figure 2. While \mathbf{F}_{base}^s learns feature representation \mathbf{h}_{base}^s ($= \mathbf{h}_{L/2+1}^s$) with no constraint, the second sub-path $\mathbf{F}_{skippable}^s$ is constrained to preserve the feature level of \mathbf{h}_{base}^s and only refine it to produce \mathbf{h}_{super}^s . Since layers in \mathbf{F}_{base}^s perform essential transformations for hierarchical feature learning, they cannot be bypassed during inference. However, since layers in $\mathbf{F}_{skippable}^s$ only refine \mathbf{h}_{base}^s , they can be skipped to save computation. If $\mathbf{F}_{skippable}^s$ is skipped, then intermediate features \mathbf{h}_{base}^s becomes the input to the next residual stage. Therefore, the overall network depth can be adjusted by choosing whether to skip $\mathbf{F}_{skippable}^s$ ($s = 1, \dots, N_s$) or not.

In Section 4.1, we show that this architectural pattern for adaptive depth networks is generally applicable to a wide range of residual networks.

3.2. Skip-Aware Self-Distillation

Preserving the feature level of \mathbf{h}_{base}^s in $\mathbf{F}_{skippable}^s$ implies, more specifically, that two feature representations \mathbf{h}_{base}^s and \mathbf{h}_{super}^s have similar distributions over training input \mathbf{X} . If \mathbf{h}_{super}^s and \mathbf{h}_{base}^s have similar distributions, skipping the sub-path $\mathbf{F}_{skippable}^s$ during inference results in minimal internal covariate shifts [25] to the following network layers. Kullback-Leibler (KL) divergence measures how different two distributions are over the same random variable, and, hence, we use Equation 2 to measure the similarity of two distributions, \mathbf{h}_{base}^s and \mathbf{h}_{super}^s , over input \mathbf{X} :

$$D_{KL}(\mathbf{h}_{super}^s || \mathbf{h}_{base}^s)_{x \in \mathbf{X}} \quad (2)$$

Algorithm 1 shows our training method, called *skip-aware self-distillation*, in which Equation 2 is included in the loss function while the largest and the smallest sub-networks of \mathbf{M} , which are called *super-net* and the *base-net*, respectively, are jointly trained¹. In Algorithm 1, the

¹Some frameworks, such as Pytorch’s distributed data parallel (DDP), do not support two consecutive forwards passes followed by a single backward pass: *super.forward* \rightarrow *base.foward* \rightarrow *loss.backward*. For such frameworks, we adapt the algorithm to *super.forward* \rightarrow *loss_super.backward* \rightarrow *base.forward* \rightarrow *loss_sub_path.backward*. The latter method has similar results and is more memory-efficient.

Algorithm 1 Training algorithm for an adaptive depth network \mathbf{M} . Two parameter-sharing sub-networks, or *super-net* and *base-net*, are jointly trained using *skip-aware self-distillation*. N_r denotes the number of residual stages.

```

1: Initialize an adaptive depth network  $\mathbf{M}$ 
2: for  $i = 1$  to  $n_{iters}$  do
3:   Get next mini-batch of data  $\mathbf{x}$  and label  $\mathbf{y}$ 
4:    $optimizer.zero\_grad()$ 
5:    $\hat{\mathbf{y}}_{super} = \mathbf{M}.forward(\mathbf{x}, skip=[False, \dots, False])$ 
6:    $loss_{super} = criterion(\mathbf{y}, \hat{\mathbf{y}}_{super})$ 
7:    $\hat{\mathbf{y}}_{base} = \mathbf{M}.forward(\mathbf{x}, skip=[True, \dots, True])$ 
8:    $loss_{base} = \sum_{s=1}^{N_r} D_{KL}(\mathbf{h}_{super}^s \| \mathbf{h}_{base}^s)$ 
     +  $D_{KL}(\hat{\mathbf{y}}_{super} \| \hat{\mathbf{y}}_{base})$ 
9:    $loss = \alpha loss_{super} + (1 - \alpha) loss_{base}$ 
10:   $loss.backward()$ 
11:   $optimizer.step()$ 
12: end for

```

forward function of the proposed adaptive depth networks \mathbf{M} accepts an extra argument, ‘skip’, that controls which residual stages skip their skippable sub-paths. For example, if \mathbf{M} has 4 residual stages, its *base-net* is selected by passing ‘skip=[True, True, True, True]’.

In steps 5 and 7, the forward passes of the super-net and the base-net are executed for the same input \mathbf{x} . Intermediate features \mathbf{h}_{super} and \mathbf{h}_{base} are also obtained during the forward passes of \mathbf{M} . In step 8, $D_{KL}(\mathbf{h}_{super}^s \| \mathbf{h}_{base}^s)$ in Equation 2 is included in the loss function $loss_{base}$. By minimizing $loss_{base}$, two feature representations \mathbf{h}_{super}^s and \mathbf{h}_{base}^s , are explicitly enforced to have similar distributions for the same input \mathbf{x} . Further, this step gives the effect of transferring the knowledge from \mathbf{h}_{super}^s to \mathbf{h}_{base}^s at every residual stage. Therefore, \mathbf{h}_{base}^s is expected to learn more compact representation from \mathbf{h}_{super}^s . The hyperparameter α controls the strength of this skip-aware self-distillation. In step 8, $D_{KL}(\hat{\mathbf{y}}_{super} \| \hat{\mathbf{y}}_{base})$ is included in the loss function for further distillation effect from the super-net to the sub-networks. Due to the architectural pattern of interleaving the mandatory and the skippable sub-paths, minimizing $D_{KL}(\hat{\mathbf{y}}_{super} \| \hat{\mathbf{y}}_{base})$ also minimizes $D_{KL}(\mathbf{h}_{super} \| \mathbf{h}_{base})$ implicitly. Experimental result shows that similar results can be achieved when only $D_{KL}(\hat{\mathbf{y}}_{super} \| \hat{\mathbf{y}}_{base})$ is used in $loss_{base}$ (Section 4.5). This implicit approach is useful when the extraction of intermediate features is tricky.

In Algorithm 1, only two sub-networks are involved for the training of \mathbf{M} , and, hence, the total training time is no greater than training two sub-networks individually. However, at test time, sub-networks with various depths can be selected on the fly by systematically skipping sub-paths in residual stages. For example, in a network with 4 residual stages, 16 ($= 2^4$) parameter-sharing sub-networks can be selected by varying the *skip* argument. In contrast, prior

adaptive networks supporting 16 parameter-sharing sub-networks need to perform 16 explicit self-distillation from the super-net to the sub-networks [20, 48, 59]. We demonstrate this result in Section 4.3.

3.3. Formal Analysis of Skippable Sub-Paths

$D_{KL}(\mathbf{h}_{super}^s \| \mathbf{h}_{base}^s)$ in Equation 2 can be trivially minimized if residual blocks in $\mathbf{F}_{skippable}^s$ learn identity functions, or $\mathbf{h}_{base}^s + \mathbf{F}_{skippable}^s(\mathbf{h}_{base}^s) = \mathbf{h}_{base}^s$. However, since the super-net is jointly trained with the loss function $loss_{super}$, the residual functions in $\mathbf{F}_{skippable}^s$ cannot simply be an identity function. Then, what do the residual functions in $\mathbf{F}_{skippable}^s$ learn during training? This can be further investigated through Taylor expansion [27]. For our adaptive depth networks, a loss function \mathcal{L} used for training the super-net can be approximated with Taylor expansion as follows:

$$\mathcal{L}(\mathbf{h}_{super}^s) = \mathcal{L}\{\mathbf{h}_{base}^s + \mathbf{F}_{skippable}^s(\mathbf{h}_{base}^s)\} \quad (3)$$

$$= \mathcal{L}\{\mathbf{h}_{base}^s + \dots + F_{L-1}(\mathbf{h}_{L-1}^s) + F_L(\mathbf{h}_L^s)\} \quad (4)$$

$$\approx \mathcal{L}\{\mathbf{h}_{base}^s + \dots + F_{L-1}(\mathbf{h}_{L-1}^s)\} + F_L(\mathbf{h}_L^s) \cdot \frac{\partial \mathcal{L}(\mathbf{h}_L^s)}{\partial \mathbf{h}_L^s} + \mathcal{O}(F_L(\mathbf{h}_L^s)) \quad (5)$$

In Equation 5, the loss function is expanded around \mathbf{h}_L^s , or $\mathbf{h}_{base}^s + \dots + F_{L-1}(\mathbf{h}_{L-1}^s)$. Only the first order term is left and all high order terms, such as $F_L(\mathbf{h}_L^s)^2 \cdot \frac{\partial^2 \mathcal{L}(\mathbf{h}_L^s)}{2\partial(\mathbf{h}_L^s)^2}$, are absorbed in $\mathcal{O}(F_L(\mathbf{h}_L^s))$.

The terms in $\mathcal{O}(F_L(\mathbf{h}_L^s))$ can be ignored if $F_L(\mathbf{h}_L^s)$ has a small magnitude. In typical residual networks, however, every layer is trained to learn new features with no constraint, and, hence, there is no guarantee that $F_L(\mathbf{h}_L^s)$ have small magnitude. In contrast, in our adaptive depth networks, the residuals in $\mathbf{F}_{skippable}^s$ are explicitly enforced to have small magnitude through the skip-aware self-distillation, and, hence, the terms in $\mathcal{O}(F_L(\mathbf{h}_L^s))$ can be ignored for the approximation. If we similarly keep expanding the loss function around \mathbf{h}_j ($j = L/2 + 1, \dots, L$) while ignoring high order terms, we obtain the following approximation:

$$\mathcal{L}(\mathbf{h}_{super}^s) \approx \mathcal{L}(\mathbf{h}_{base}^s) + \sum_{j=L/2+1}^L F_j(\mathbf{h}_j^s) \cdot \frac{\partial \mathcal{L}(\mathbf{h}_j^s)}{\partial \mathbf{h}_j^s} \quad (6)$$

In Equation 6, minimizing the loss $\mathcal{L}(\mathbf{h}_{super}^s)$ during training drives $F_j(\mathbf{h}_j^s)$ ($j = L/2 + 1, \dots, L$) in the negative half space of $\frac{\partial \mathcal{L}(\mathbf{h}_j^s)}{\partial \mathbf{h}_j^s}$ to minimize the dot product between $F_j(\mathbf{h}_j^s)$ and $\frac{\partial \mathcal{L}(\mathbf{h}_j^s)}{\partial \mathbf{h}_j^s}$. This implies that every residual function in $\mathbf{F}_{skippable}^s$ is optimized to learn a function that has a similar effect to gradient descent:

$$F_j(\mathbf{h}_j^s) \simeq - \frac{\partial \mathcal{L}(\mathbf{h}_j^s)}{\partial \mathbf{h}_j^s} \quad (j = L/2 + 1, \dots, L) \quad (7)$$

In other words, the residual functions in the skippable sub-paths reduce the loss $\mathcal{L}(\mathbf{h}_{base}^s)$ iteratively during inference while preserving the feature distribution of \mathbf{h}_{base}^s .

Considering this result, we can conjecture that, with our architectural pattern and training method, layers in $\mathbf{F}_{skippable}^s$ learn functions that refine input features \mathbf{h}_{base}^s iteratively for better inference accuracy while minimally changing the distribution of \mathbf{h}_{base}^s . Therefore, skipping $\mathbf{F}_{skippable}^s$ only slightly reduces prediction accuracy.

3.4. Skip-aware Batch Normalization

Originally, batch normalization (BN) [25] was proposed to handle internal covariate shift during training non-adaptive networks by normalizing features. In our adaptive depth networks, however, internal covariate shifts can occur during inference in mandatory sub-paths if different sub-networks are selected. To handle potential internal covariate shifts, switchable BN operators, called *skip-aware BNs*, are used in mandatory sub-paths. For example, at each residual stage, two sets of BNs are available for the mandatory sub-path, and they are switched depending on whether its skippable sub-path is skipped or not.

The effectiveness of switchable BNs has been demonstrated in networks with adaptive widths [48, 57] and adaptive resolutions [62]. However, in previous adaptive networks, N sets of switchable BNs are required in every layer to support N parameter-sharing sub-networks. Such a large number of switchable BNs not only requires more parameters, but also makes the training process complicated since N sets of switchable BNs need to be trained iteratively during training. In contrast, in our adaptive depth networks, every mandatory sub-path needs only two sets of switchable BNs, regardless of the number of supported sub-networks. This reduced number of switchable BNs significantly simplifies the training process as shown in Algorithm 1. Furthermore, the amount of parameters for skip-aware BNs is negligible. For instance, in ResNet50, skip-aware BNs increase the parameters by 0.07%.

Transformers [34, 44] exploit layer normalization (LN) instead of BNs and naive replacement of LNs to BNs incurs instability during training [54]. Therefore, for our adaptive depth transformers, we apply switchable LN operators in mandatory sub-paths instead of switchable BNs.

4. Experiments

To demonstrate the generality and effectiveness of our approach for adaptive depth networks, we conduct experiments on various networks and vision tasks.

4.1. Networks

We use four representative residual networks as base models to apply the proposed architecture pattern in Section 3.1:

Table 1. Results on ImageNet. Individual networks with the suffix ‘-Base’ have the same depths as the base-nets of corresponding adaptive depth networks. Latency is measured on an RTX 3090 (batch size = 64).

Model	Params (M)	FLOPs (G)	Acc@1 (%)	Latency (msec)
ResNet50-ADN (super-net)	25.58	4.11	77.6	43.2
ResNet50-ADN (base-net)		2.58	76.1	27.6
ResNet50 (individual)	25.56	4.11	76.7	43.2
ResNet50-Base (individual)	17.11	2.58	75.0	27.6
MV2-ADN (super-net)	3.72	0.32	72.7	15.5
MV2-ADN (base-net)		0.25	70.7	13.2
MV2 (individual)	3.50	0.32	72.1	15.5
MV2-Base (individual)	2.99	0.25	70.7	13.2
ViT-b/16-ADN (super-net)	86.59	17.58	81.3	138.6
ViT-b/16-ADN (base-net)		11.76	79.4	90.7
ViT-b/16 (individual)	86.57	17.58	81.1	138.6
ViT-b/16-Base (individual)	67.70	11.76	78.7	90.7
Swin-T-ADN (super-net)	28.30	4.49	81.8	74.4
Swin-T-ADN (base-net)		2.69	78.7	39.9
Swin-T (individual)	28.29	4.49	81.5	74.4
Swin-T-Base (individual)	15.63	2.69	78.6	39.9

MobileNet V2 [38] is a lightweight CNN model, ResNet [16] is a larger CNN model, and ViT [5] and Swin-T [34] are representative vision transformers. All base models except ViT have 4 residual stages, each with 2 ~ 6 (residual or encoder) blocks. So, according to the proposed architectural pattern, every residual stage is evenly divided into 2 sub-paths for depth adaptation. Since ViT does not define residual stages, we divide 12 encoder blocks into 4 groups, resembling other residual networks, and designate the last encoder block of each group as a skippable sub-path.

We use the suffix ‘-ADN’ to denote our adaptive depth networks. Since our adaptive depth networks have many parameter-sharing sub-networks in a single network, we indicate which sub-network is used for evaluation in parenthesis, e.g., ResNet50-ADN (super-net). For our sub-networks, boolean values are also used to indicate in which residual stages the sub-paths are skipped. For example, ResNet50-ADN (base-net) is equivalent to ResNet50-ADN (TTTT).

4.2. ImageNet Classification

We evaluate our method on ILSVRC2012 dataset [37] that has 1000 classes. The dataset consists of 1.28M training and 50K validation images. For CNN models, we follow most training settings in the original papers [16, 38], except that ResNet models are trained for 150 epochs. ViT and Swin-T are trained for 300 epochs, following DeiT’s training recipe [1, 42]. However, in Swin-T-ADN, we disable stochastic depths [23] for the base-net since the strategy of random dropping of residual blocks conflicts with our approach to

skipping sub-paths. For fair comparison, our adaptive depth networks and corresponding individual networks are trained in the same training settings. The hyperparameter α in Algorithm 1 is set to 0.5 for all networks.

The results in Table 1 show that our adaptive depth networks outperform individual counterpart networks even though our sub-networks share parameters in a single network. Further, our results with vision transformers demonstrate that our approach is generally applicable to residual networks and compatible with their state-of-the-art training techniques such as DeiT’s training recipe [42]. We conjecture that this performance improvement results from effective distillation of knowledge from \mathbf{h}_{super}^s to \mathbf{h}_{base}^s at each residual stage and the iterative feature refinement at skip-able sub-paths, shown in Equation 7.

In Table 2 and Figure 3, several state-of-the-art efficient inference methods and dynamic networks are compared with our sub-networks of adaptive depth networks. The result demonstrates that our adaptive depth networks match or outperform many state-of-the-art static and dynamic networks across varying depth ranges.

In Figure 3, sub-networks of ResNet50-ADN are compared to the counterpart individual ResNets of equivalent depths. In particular, it should be noted that ResNets trained with knowledge distillation in the same training settings has worse performance than individual ResNets trained without knowledge distillation. As reported in previous works, successful knowledge distillation requires a patient and long training [2], and straightforward knowledge distillation using ImageNet does not improve the performance of student models [4, 60]. In contrast, our ResNet50-ADN trained with skip-aware self-distillation achieves better performance than counterpart ResNets. This demonstrates that the high performance of adaptive depth networks does not simply come from the distillation effect, but from the effective combination of the proposed architectural pattern and the skip-aware self-distillation strategy.

4.3. Training Time

One important advantage of our approach is that our adaptive depth networks require significantly shorter training time than other adaptive networks. Table 3 shows that training our ResNet50-ADN takes similar time to train two individual networks combined. In contrast, the compared adaptive networks requires much longer training time than ours. MSDNet [24] represents adaptive depth networks with multiple early-exiting branches and classifiers. Skip-Net [50] represents input-dependent dynamic networks that drop layers for ‘easy’ inputs. In S-ResNet50 [59], 4 sub-networks with varying widths are trained through iterative self-distillation from its super-net.

Despite significantly shorter training time is required, our adaptive depth networks can support various sub-

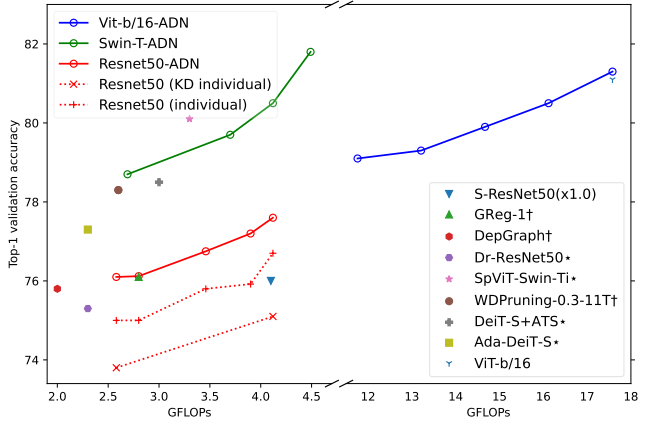


Figure 3. Comparison with various approaches on ImageNet. Sub-networks of our adaptive depth networks match or outperform other approaches on ImageNet. ResNet50 (individual) shows individual networks that have equivalent network depths as the sub-networks of ResNet50-ADN. ResNet50 (KD individual) shows individual networks trained using knowledge distillation from pre-trained Pytorch ResNet50. In legend, † denotes static compression methods, and * denotes input-dependent dynamic networks.

Table 2. Our base-nets are compared with state-of-the-art efficient inference methods for various networks. † denotes static compression methods, * denotes width-adaptation networks, and * denotes input-dependent dynamic networks. Note that many of these state-of-the-art methods exploit various non-canonical training techniques, such as iterative retraining and post-processing, while our base-nets are selected from adaptive depth networks without any fine-tuning.

Model	FLOPs	↓FLOPs	Acc@1
GReg-1 [49]†	2.8G	33%	76.1%
DR-ResNet50 ($\alpha=2.0$) [62]*	2.3G	44%	75.3%
DepGraph [7]†	2.0G	51%	75.8%
ResNet50-ADN (base-net)	2.6G	37%	76.1%
AlphaNet-0.75x [48] *	0.21G	34%	70.5%
MV2-ADN (base-net)	0.25G	22%	70.7%
Ada-DeiT-S [35]*	2.3G	-	77.3%
WDPPruning-0.3-11 [56]†	2.6G	-	78.3%
DeiT-S+ATS (not fine-tuned) [8]*	3.0G	-	78.5%
SPViT-Swin-Ti [28]*	3.3G	27%	80.1%
Swin-T-ADN (base-net)	2.7G	40%	78.7%

networks at test time. Figure 4-(left) shows the performance of ResNet50-ADN when its depth is varied at test time. Among them, only the super-net and the base-net are explicitly trained in Algorithm 1. Other sub-networks are selected on the fly at test time by skipping sub-paths in varying number of residual stages. Although these sub-networks are not trained explicitly, they show graceful degradation of performance as the depth of sub-networks becomes gradually shallower. However, although ResNet50-ADN support 2^4 sub-networks in theory, Figure 4-(right) shows that

Table 3. Training time (1 epoch), measured on a Nvidia RTX 4090 (batch size = 128). All compared models are based on ResNet50 or have similar FLOPs and depths.

Model	Training time (min)	# of sub-networks
ResNet50	32.9	1
ResNet50-Base	22.7	1
ResNet50-ADN (ours)	54.7	2 ⁴ (varying depths)
MSDNet [24]	67.1	9 (early-exit branches)
S-ResNet50 [59]	82.5	4 (varying widths)
SkipNet [50]	90.6	dynamic depths

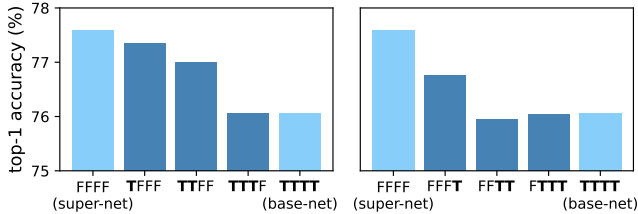


Figure 4. Validation accuracy of our sub-networks of varying depths. The boolean values below the bars indicate the residual stages where the sub-paths are skipped.

some sub-networks are more useful than the others. For instance, even though ResNet50-ADN(TFFF) and ResNet50-ADN(FFFT) have the same network depths, ResNet50-ADN(TFFF) has about 0.58% higher top-1 accuracy. This result shows that skipping sub-paths in later stages is more detrimental to the performance in general.

4.4. Performance on Devices

Figure 5 shows the performance of adaptive networks in an actual device. The inference latency and energy consumption of ResNet50-ADN is compared to S-ResNet50 [59], a representative width-adaptation network. The result shows that depth-adaptation of ResNet50-ADN is highly effective in accelerating inference speeds and reducing energy consumption. For example, in ResNet50-ADN, reducing FLOPs by 38% through depth adaptation reduces both inference latency and energy consumption by 35%. In contrast, even though S-ResNet50 can reduce FLOPs by up to 93% by adjusting its width, it only achieves up to 9% acceleration in practice.

4.5. Ablation Study

We conduct ablation study on ImageNet classification to investigate the influence of two key components of the proposed adaptive depth networks: (1) skip-aware self-distillation and (2) skip-aware BN/LNs. When our skip-aware self-distillation is not applied, the loss in Algorithm 1 is modified to $loss = \frac{1}{2}\{criterion(\mathbf{y}, \hat{\mathbf{y}}_{super}) + criterion(\mathbf{y}, \hat{\mathbf{y}}_{base})\}$ for joint training of the super-net and the base-net. Table 4 shows the results. For ResNet50,

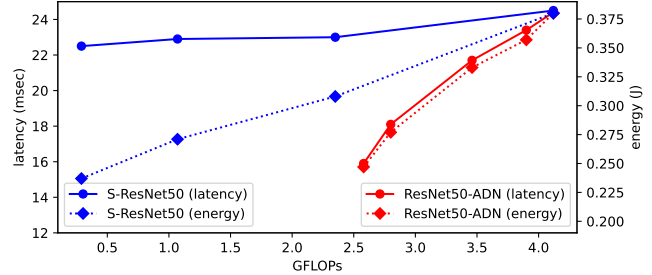


Figure 5. Inference latency and energy consumption of adaptive networks, measured on Nvidia Jetson Orin Nano (batch size = 1). Although adjusting the network width can support a much wider FLOPs adaptation range, depth adaptation of ResNet50-ADN is more effective for actual inference acceleration and saving energy.

when neither of them is applied, the inference accuracy of the super-net and the base-net is significantly lower than individual networks by 1.5% and 2.8%, respectively. This result shows the difficulty of joint training sub-networks for adaptive networks. When one of the two components is applied individually, the performance is still slightly worse than individual networks'. In the third row, when both skip-aware self-distillation and skip-aware BNs are applied together, ResNet50-ADN achieves significantly better performance than individual networks, both in the super-net and the base-net. Finally, the last row shows the result when only $D_{KL}(\hat{\mathbf{y}}_{super} || \hat{\mathbf{y}}_{base})$ is used for skip-aware self-distillation. Without explicit distillation of intermediate features, slightly lower performance is observed in the base-net. The results with ViT-b/32 show that switchable layer normalization has similar effect in vision transformers.

4.6. Visual Analysis of Sub-Paths

To investigate how our training method affects feature representations in the mandatory and the skippable sub-paths, we visualize the activation of 3rd residual stage of ResNet50-ADN using Grad-CAM [39]. The 3rd residual stage of ResNet50-ADN has 6 residual blocks and the last three blocks are skippable. In Figure 6-(a), the activation regions of original ResNet50 changes gradually across all consecutive blocks. In contrast, in Figure 6-(b), ResNet50-ADN (super-net) manifests very different activation regions in two sub-paths. In the first three residual blocks, we can observe lots of hot activation regions in wide areas, suggesting active learning of new level features. In contrast, significantly less activation regions are found in the skippable last three blocks and they are gradually concentrated around the target object, demonstrating the refinement of learned features. Further, in Figure 6-(c), we can observe that the final activation map of the ResNet50 (base-net) is very similar to the super-net's final activation map in Figure 6-(b). This implies that they have similar distributions for the same inputs, as suggested in Section 3.3.

Table 4. Ablation analysis with ResNet50-ADN and ViT-b/32-ADN. Applied components are checked. In the last row, only D_{KL} with softmax outputs is used for the skip-aware self-distillation. \downarrow and \uparrow in parentheses are comparisons to individual networks.

Skip-aware self-distillation	Skip-aware BNs / LNs	ResNet50 Acc@1		ViT-b/32 Acc@1	
		Super-net	Base-net	Super-net	Base-net
		75.2% (\downarrow 1.5%)	72.2% (\downarrow 2.8%)	75.7% (\downarrow 0.2%)	74.1% (\uparrow 0.3%)
O		76.1% (\downarrow 0.6%)	74.9% (\downarrow 0.1%)	76.4% (\uparrow 0.5%)	74.3% (\uparrow 0.5%)
	O	76.6% (\downarrow 0.1%)	75.1% (\uparrow 0.1%)	76.0% (\uparrow 0.1%)	74.3% (\uparrow 0.5%)
O	O	77.6% (\uparrow 0.9%)	76.1% (\uparrow 1.1%)	76.6% (\uparrow 0.8%)	74.3% (\uparrow 0.5%)
Δ	O	77.6% (\uparrow 0.9%)	75.9% (\uparrow 0.9%)		

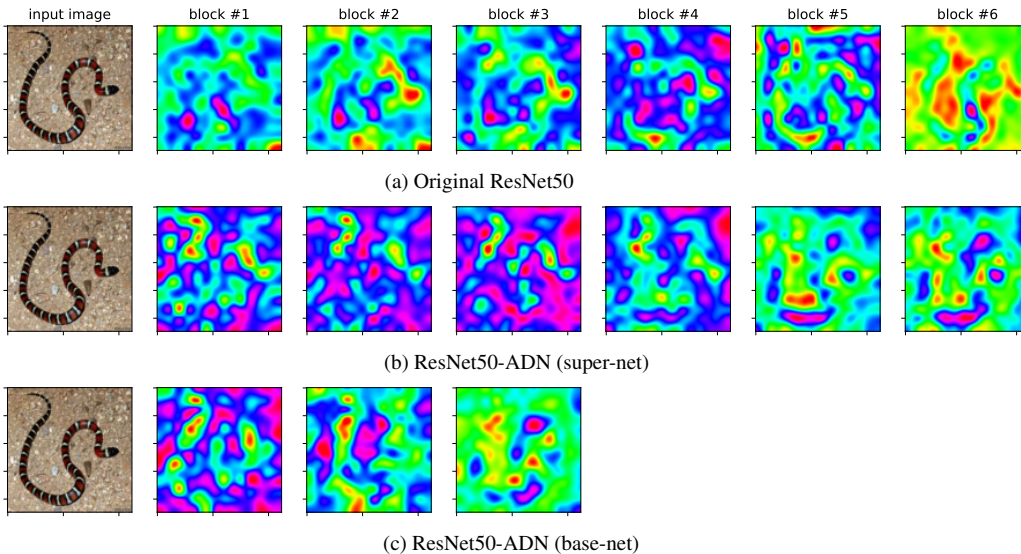


Figure 6. Class Activation Maps of the 3rd residual stages of ResNet50s. **(a)** Original ResNet50’s activation regions change gradually across all blocks. **(b)** In ResNet50-ADN (super-net), the first 3 blocks have extensive hot activation regions, implying active learning of new level features. In contrast, the skipable last 3 blocks have far less activation regions and they are gradually refined around the target. **(c)** The base-net’s final activation map is very similar to super-net’s final activation map, implying that they are at the same feature level.

4.7. Object Detection and Instance Segmentation

In order to investigate the generalization ability of our approach, we use MS COCO 2017 datasets on object detection and instance segmentation tasks using representative detectors. We compare individual ResNet50 and our adaptive depth ResNet50-ADN as backbone networks of the detectors. For training of detectors, we use Algorithm 1 with slight adaptation. For object detection, the intermediate features \mathbf{h}_{base}^s and $\mathbf{h}_{super}^s (s = 1..N_r)$ can be obtained directly from backbone network’s feature pyramid networks (FPN) [32], and, hence, a wrapper function is not required to extract intermediate features. All networks are trained on train2017 for 12 epochs from ImageNet pretrained weights, following the training settings suggested in [32]. Table 5 shows the results on val2017 containing 5000 images. Our adaptive depth backbone networks still outperform individual static backbone networks in terms of COCO’s standard metric AP.

5. Conclusions

We propose an architectural pattern for adaptive depth networks and its training method that renders selected sub-paths of the network to incur minimal performance degradation even if they are skipped during inference. Our approach does not train a fixed set of sub-networks iteratively, and, hence significantly shorter training time is required than previous adaptive networks. However, once deployed on devices, it can instantly construct sub-networks of various depths to provide various accuracy-efficiency trade-offs in a single network. We show formally that the proposed architectural pattern and training method reduces overall prediction errors while minimizing the impact of skipping sub-paths. We also empirically demonstrate the generality and effectiveness of our approach using representative convolutional neural networks and vision transformers.

Table 5. Object detection and instance segmentation results on MS COCO dataset.

Detector	Backbone	FLOPs	Individual Networks		ResNet50-ADN (ours)	
			Box AP	Mask AP	Box AP	Mask AP
Faster-RCNN [36]	ResNet50 ResNet50-Base	207.07G 175.66G	36.4 32.4		37.8 34.0	
Mask-RCNN [17]	ResNet50 ResNet50-Base	260.14G 228.73G	37.2 32.7	34.1 29.9	38.3 34.1	34.1 31.2

References

- [1] Image classification reference training scripts in PyTorch, <https://github.com/pytorch/vision/tree/main/references/classification>, 2023. **5**
- [2] Lucas Beyer, Xiaoohua Zhai, Amélie Royer, Larisa Markeeva, Rohan Anil, and Alexander Kolesnikov. Knowledge distillation: A good teacher is patient and consistent. In *Conference on Computer Vision and Pattern Recognition (CVPR)*, pages 10925–10934, 2022. **6**
- [3] Lucas Beyer, Pavel Izmailov, Alexander Kolesnikov, Mathilde Caron, Simon Kornblith, Xiaohua Zhai, Matthias Minderer, Michael Tschannen, Ibrahim Alabdulmohsin, and Filip Pavetic. Flexivit: One model for all patch sizes. In *Conference on Computer Vision and Pattern Recognition (CVPR)*, 2023. **2**
- [4] Jang Hyun Cho and Bharath Hariharan. On the efficacy of knowledge distillation. In *International Conference on Computer Vision (ICCV)*, pages 4794–4802, 2019. **6**
- [5] Alexey Dosovitskiy, Lucas Beyer, Alexander Kolesnikov, Dirk Weissenborn, Xiaohua Zhai, Thomas Unterthiner, Mostafa Dehghani, Matthias Minderer, Georg Heigold, Sylvain Gelly, Jakob Uszkoreit, and Neil Houlsby. An image is worth 16x16 words: Transformers for image recognition at scale. In *International Conference on Learning Representations (ICLR)*, 2021. **2, 5**
- [6] Angela Fan, Edouard Grave, and Armand Joulin. Reducing transformer depth on demand with structured dropout. In *International Conference on Learning Representations (ICLR)*, 2020. **1, 2**
- [7] Gongfan Fang, Xinyin Ma, Mingli Song, Michael Bi Mi, and Xinchao Wang. Depgraph: Towards any structural pruning. In *Conference on Computer Vision and Pattern Recognition (CVPR)*, pages 16091–16101, 2023. **6**
- [8] Mohsen Fayyaz, Soroush Abbasi Koohpayegani, Farnoush Rezaei Jafari, Sunando Sengupta, Hamid Reza Vaezi Joze, Eric Sommerlade, Hamed Pirsiavash, and Jürgen Gall. Adaptive token sampling for efficient vision transformers. In *European Conference on Computer Vision (ECCV)*, pages 396–414, 2022. **2, 6**
- [9] Michael Figurnov, Maxwell D Collins, Yukun Zhu, Li Zhang, Jonathan Huang, Dmitry Vetrov, and Ruslan Salakhutdinov. Spatially adaptive computation time for residual networks. In *Conference on Computer Vision and Pattern Recognition (CVPR)*, pages 1039–1048, 2017. **2**
- [10] Chengyue Gong, Dilin Wang, Meng Li, Xinlei Chen, Zhicheng Yan, Yuandong Tian, qiang liu, and Vikas Chandra. NASvit: Neural architecture search for efficient vision transformers with gradient conflict aware supernet training. In *International Conference on Learning Representations (ICLR)*, 2022. **1**
- [11] Klaus Greff, Rupesh K Srivastava, and Jürgen Schmidhuber. Highway and residual networks learn unrolled iterative estimations. In *International Conference on Learning Representations (ICLR)*, 2016. **2, 3**
- [12] Q. Guo, Z. Yu, Y. Wu, D. Liang, H. Qin, and J. Yan. Dynamic recursive neural network. In *2019 IEEE/CVF Conference on Computer Vision and Pattern Recognition (CVPR)*, pages 5142–5151, 2019. **2**
- [13] Kai Han, Yunhe Wang, Qi Tian, Jianyuan Guo, Chunjing Xu, and Chang Xu. Ghostnet: More features from cheap operations. In *IEEE/CVF Conference on Computer Vision and Pattern Recognition (CVPR)*, 2020. **1**
- [14] Song Han, Huizi Mao, and William J. Dally. Deep compression: Compressing deep neural network with pruning, trained quantization and Huffman coding. In *International Conference on Learning Representations (ICLR)*, 2016. **1**
- [15] Y. Han, G. Huang, S. Song, L. Yang, H. Wang, and Y. Wang. Dynamic neural networks: A survey. *IEEE Transactions on Pattern Analysis and Machine Intelligence*, 44(11):7436–7456, 2022. **2**
- [16] Kaiming He, Xiangyu Zhang, Shaoqing Ren, and Jian Sun. Deep residual learning for image recognition. In *Conference on Computer Vision and Pattern Recognition (CVPR)*, pages 770–778, 2016. **2, 3, 5**
- [17] Kaiming He, Georgia Gkioxari, Piotr Dollár, and Ross Girshick. Mask r-cnn. In *International Conference on Computer Vision (ICCV)*, pages 2961–2969, 2017. **9**
- [18] Byeongho Heo, Sangdoon Yun, Dongyoon Han, Sanghyuk Chun, Junsuk Choe, and Seong Joon Oh. Rethinking spatial dimensions of vision transformers. In *International Conference on Computer Vision (ICCV)*, 2021. **2**
- [19] Geoffrey Hinton, Oriol Vinyals, and Jeff Dean. Distilling the knowledge in a neural network. *arXiv preprint arXiv:1503.02531*, 2015. **1**
- [20] Lu Hou, Zhiqi Huang, Lifeng Shang, Xin Jiang, Xiao Chen, and Qun Liu. Dynabert: Dynamic bert with adaptive width and depth. *Conference on Neural Information Processing Systems (NeurIPS)*, 33, 2020. **1, 2, 4**
- [21] Andrew G Howard, Menglong Zhu, Bo Chen, Dmitry Kalenichenko, Weijun Wang, Tobias Weyand, Marco Andreetto, and Hartwig Adam. Mobilenets: Efficient convolutional neural networks for mobile vision applications. *arXiv preprint arXiv:1704.04861*, 2017. **1**
- [22] Hanzhang Hu, Debadeepta Dey, Martial Hebert, and J Andrew Bagnell. Learning anytime predictions in neural net-

- works via adaptive loss balancing. In *Proceedings of the AAAI Conference on Artificial Intelligence*, pages 3812–3821, 2019. [2](#)
- [23] Gao Huang, Yu Sun, Zhuang Liu, Daniel Sedra, and Kilian Q Weinberger. Deep networks with stochastic depth. In *European Conference on Computer Vision (ECCV)*, pages 646–661. Springer, 2016. [2](#), [3](#), [5](#)
- [24] Gao Huang, Danlu Chen, Tianhong Li, Felix Wu, Laurens van der Maaten, and Kilian Weinberger. Multi-scale dense networks for resource efficient image classification. In *International Conference on Learning Representations (ICLR)*, 2018. [1](#), [2](#), [6](#), [7](#)
- [25] Sergey Ioffe and Christian Szegedy. Batch normalization: Accelerating deep network training by reducing internal covariate shift. In *International Conference on Machine Learning (ICML)*, pages 448–456. PMLR, 2015. [3](#), [5](#)
- [26] Benoit Jacob, Skirmantas Kligys, Bo Chen, Menglong Zhu, Matthew Tang, Andrew Howard, Hartwig Adam, and Dmitry Kalenichenko. Quantization and training of neural networks for efficient integer-arithmetic-only inference. In *Conference on Computer Vision and Pattern Recognition (CVPR)*, 2018. [1](#)
- [27] Stanisław Jastrzebski, Devansh Arpit, Nicolas Ballas, Vikas Verma, Tong Che, and Yoshua Bengio. Residual connections encourage iterative inference. In *International Conference on Learning Representations (ICLR)*, 2018. [2](#), [3](#), [4](#)
- [28] Zhenglun Kong, Peiyan Dong, Xiaolong Ma, Xin Meng, Wei Niu, Mengshu Sun, Xuan Shen, Geng Yuan, Bin Ren, Hao Tang, Minghai Qin, and Yanzhi Wang. Spvit: Enabling faster vision transformers via latency-aware soft token pruning. In *European Conference on Computer Vision (ECCV)*, pages 620–640, 2022. [6](#)
- [29] Changlin Li, Guangrun Wang, Bing Wang, Xiaodan Liang, Zhihui Li, and Xiaojun Chang. Dynamic slimmable network. In *Conference on Computer Vision and Pattern Recognition (CVPR)*, pages 8607–8617, 2021. [2](#)
- [30] Hao Li, Hong Zhang, Xiaojuan Qi, Ruigang Yang, and Gao Huang. Improved techniques for training adaptive deep networks. In *International Conference on Computer Vision (ICCV)*, pages 1891–1900, 2019. [1](#), [2](#)
- [31] Yanwei Li, Lin Song, Yukang Chen, Zeming Li, Xiangyu Zhang, Xingang Wang, and Jian Sun. Learning dynamic routing for semantic segmentation. In *Conference on Computer Vision and Pattern Recognition (CVPR)*, 2020. [2](#)
- [32] Tsung-Yi Lin, Piotr Dollar, Ross Girshick, Kaiming He, Bharath Hariharan, and Serge Belongie. Feature pyramid networks for object detection. In *Conference on Computer Vision and Pattern Recognition (CVPR)*, 2017. [8](#)
- [33] Zechun Liu, Haoyuan Mu, Xiangyu Zhang, Zichao Guo, Xin Yang, Kwang-Ting Cheng, and Jian Sun. Metapruning: Meta learning for automatic neural network channel pruning. In *International Conference on Computer Vision (ICCV)*, pages 3296–3305, 2019. [1](#)
- [34] Ze Liu, Yutong Lin, Yue Cao, Han Hu, Yixuan Wei, Zheng Zhang, Stephen Lin, and Baining Guo. Swin transformer: Hierarchical vision transformer using shifted windows. In *International Conference on Computer Vision (ICCV)*, 2021. [2](#), [3](#), [5](#)
- [35] L. Meng, H. Li, B. Chen, S. Lan, Z. Wu, Y. Jiang, and S. Lim. Adavit: Adaptive vision transformers for efficient image recognition. In *Conference on Computer Vision and Pattern Recognition (CVPR)*, pages 12299–12308, 2022. [2](#), [6](#)
- [36] Shaoqing Ren, Kaiming He, Ross Girshick, and Jian Sun. Faster r-cnn: Towards real-time object detection with region proposal networks. *IEEE Transactions on Pattern Analysis and Machine Intelligence*, 2017. [9](#)
- [37] Olga Russakovsky, Jia Deng, Hao Su, Jonathan Krause, Sanjeev Satheesh, Sean Ma, Zhiheng Huang, Andrej Karpathy, Aditya Khosla, Michael Bernstein, et al. Imagenet large scale visual recognition challenge. *International journal of computer vision*, 115(3):211–252, 2015. [5](#)
- [38] Mark Sandler, Andrew Howard, Menglong Zhu, Andrey Zhmoginov, and Liang-Chieh Chen. Mobilenetv2: Inverted residuals and linear bottlenecks. In *Conference on Computer Vision and Pattern Recognition (CVPR)*, pages 4510–4520, 2018. [2](#), [5](#)
- [39] Ramprasaath R Selvaraju, Michael Cogswell, Abhishek Das, Ramakrishna Vedantam, Devi Parikh, and Dhruv Batra. Grad-cam: Visual explanations from deep networks via gradient-based localization. In *International Conference on Computer Vision (ICCV)*, pages 618–626, 2017. [7](#)
- [40] Karen Simonyan and Andrew Zisserman. Very deep convolutional networks for large-scale image recognition. In *3th International Conference on Learning Representations (ICLR)*, 2015. [3](#)
- [41] Mingxing Tan and Quoc Le. Efficientnet: Rethinking model scaling for convolutional neural networks. In *International Conference on Machine Learning (ICML)*, pages 6105–6114. PMLR, 2019. [2](#)
- [42] Hugo Touvron, Matthieu Cord, Matthijs Douze, Francisco Massa, Alexandre Sablayrolles, and Hervé Jégou. Training data-efficient image transformers & distillation through attention. *arXiv preprint*, 2020. [5](#), [6](#)
- [43] Hugo Touvron, Matthieu Cord, Maxime Oquab, Piotr Bojanowski, Jakob Verbeek, and Hervé Jégou. Co-training 2l submodels for visual recognition. In *Conference on Computer Vision and Pattern Recognition (CVPR)*, 2023. [1](#)
- [44] Ashish Vaswani, Noam Shazeer, Niki Parmar, Jakob Uszkoreit, Llion Jones, Aidan N Gomez, Łukasz Kaiser, and Illia Polosukhin. Attention is all you need. In *Conference on Neural Information Processing Systems (NeurIPS)*, 2017. [1](#), [2](#), [5](#)
- [45] Andreas Veit and Serge Belongie. Convolutional networks with adaptive inference graphs. In *European Conference on Computer Vision (ECCV)*, pages 3–18, 2018. [2](#)
- [46] Andreas Veit, Michael J Wilber, and Serge Belongie. Residual networks behave like ensembles of relatively shallow networks. *Conference on Neural Information Processing Systems (NeurIPS)*, 29:550–558, 2016. [2](#)
- [47] Chengcheng Wan, Henry Hoffmann, Shan Lu, and Michael Maire. Orthogonalized sgd and nested architectures for anytime neural networks. In *International Conference on Machine Learning (ICML)*, pages 9807–9817. PMLR, 2020. [1](#), [2](#)
- [48] Dilin Wang, Chengyue Gong, Meng Li, Qiang Liu, and Vikas Chandra. Alphanet: Improved training of supernet

- with alpha-divergence. In *International Conference on Machine Learning (ICML)*, pages 10760–10771. PMLR, 2021. [1](#), [2](#), [4](#), [5](#), [6](#)
- [49] Huan Wang, Can Qin, Yulun Zhang, and Yun Fu. Neural pruning via growing regularization. In *International Conference on Learning Representations (ICLR)*, 2021. [6](#)
- [50] Xin Wang, Fisher Yu, Zi-Yi Dou, Trevor Darrell, and Joseph E Gonzalez. Skipnet: Learning dynamic routing in convolutional networks. In *European Conference on Computer Vision (ECCV)*, pages 409–424, 2018. [2](#), [6](#), [7](#)
- [51] Zuxuan Wu, Tushar Nagarajan, Abhishek Kumar, Steven Rennie, Larry S Davis, Kristen Grauman, and Rogerio Feris. Blockdrop: Dynamic inference paths in residual networks. In *Conference on Computer Vision and Pattern Recognition (CVPR)*, pages 8817–8826, 2018. [2](#)
- [52] Qizhe Xie, Minh-Thang Luong, Eduard Hovy, and Quoc V Le. Self-training with noisy student improves imagenet classification. In *Conference on Computer Vision and Pattern Recognition (CVPR)*, pages 10687–10698, 2020. [2](#), [3](#)
- [53] Le Yang, Yizeng Han, Xi Chen, Shiji Song, Jifeng Dai, and Gao Huang. Resolution adaptive networks for efficient inference. In *Proceedings of the IEEE Conference on Computer Vision and Pattern Recognition*, 2020. [2](#)
- [54] Zhuliang Yao, Yue Cao, Yutong Lin, Ze Liu, Zheng Zhang, and Han Hu. Leveraging batch normalization for vision transformers. In *2021 IEEE/CVF International Conference on Computer Vision Workshops (ICCVW)*, pages 413–422, 2021. [5](#)
- [55] Hongxu Yin, Arash Vahdat, Jose M. Alvarez, Arun Mallya, Jan Kautz, and Pavlo Molchanov. A-ViT: Adaptive tokens for efficient vision transformer. In *Conference on Computer Vision and Pattern Recognition (CVPR)*, pages 10809–10818, 2022. [2](#)
- [56] Fang Yu, Kun Huang, Meng Wang, Yuan Cheng, Wei Chu, and Li Cui. Width & depth pruning for vision transformers. *Proceedings of the AAAI Conference on Artificial Intelligence*, 36(3):3143–3151, 2022. [6](#)
- [57] Jiahui Yu and Thomas Huang. Autoslim: Towards one-shot architecture search for channel numbers. *arXiv preprint*, 2019. [5](#)
- [58] Jiahui Yu and Thomas S Huang. Universally slimable networks and improved training techniques. In *International Conference on Computer Vision (ICCV)*, pages 1803–1811, 2019. [2](#)
- [59] Jiahui Yu, Linjie Yang, Ning Xu, Jianchao Yang, and Thomas Huang. Slimmable neural networks. In *International Conference on Learning Representations (ICLR)*, 2018. [1](#), [2](#), [4](#), [6](#), [7](#)
- [60] Sergey Zagoruyko and Nikos Komodakis. Paying more attention to attention: Improving the performance of convolutional neural networks via attention transfer. In *5th International Conference on Learning Representations, ICLR*, 2017. [6](#)
- [61] Linfeng Zhang, Jiebo Song, Anni Gao, Jingwei Chen, Chenglong Bao, and Kaisheng Ma. Be your own teacher: Improve the performance of convolutional neural networks via self distillation. In *International Conference on Computer Vision (ICCV)*, pages 3713–3722, 2019. [2](#)
- [62] Mingjian Zhu, Kai Han, Enhua Wu, Qiulin Zhang, Ying Nie, Zhenzhong Lan, and Yunhe Wang. Dynamic resolution network. In *Conference on Neural Information Processing Systems (NeurIPS)*, pages 10985–10998, 2021. [5](#), [6](#)